

The link between mass distribution and starbursts in dwarf galaxies^{*}

Kristen B. W. McQuinn^{1†}, Federico Lelli,² Evan D. Skillman,¹
 Andrew E. Dolphin,³ Stacy S. McGaugh,² Benjamin F. Williams⁴

¹*Minnesota Institute for Astrophysics, School of Physics and Astronomy, 116 Church Street, S.E., University of Minnesota, Minneapolis, MN 55455*

²*Department of Astronomy, Case Western Reserve University, Cleveland, OH 44106*

³*Raytheon Company, 1151 E. Hermans Road, Tucson, AZ 85756*

⁴*Department of Astronomy, Box 351580, University of Washington, Seattle, WA 98195*

ABSTRACT

Recent studies have shown that starburst dwarf galaxies have steeply rising rotation curves in their inner parts, pointing to a close link between the intense star formation and a centrally concentrated mass distribution (baryons and dark matter). More quiescent dwarf irregulars typically have slowly rising rotation curves, although some “compact” irregulars with steep, inner rotation curves exist. We analyze archival Hubble Space Telescope images of two nearby “compact” irregular galaxies (NGC 4190 and NGC 5204), which were selected solely on the basis of their dynamical properties and their proximity. We derive their recent star-formation histories by fitting color-magnitude diagrams of resolved stellar populations, and find that the star-formation properties of both galaxies are consistent with those of known starburst dwarfs. Despite the small sample, this strongly reinforces the notion that the starburst activity is closely related to the inner shape of the potential well.

Key words: galaxies: dwarf – galaxies: starburst – galaxies: irregulars – galaxies: kinematics and dynamics

1 CONNECTING STAR-FORMATION CHARACTERISTICS AND MASS DISTRIBUTIONS

Despite numerous and extensive investigations, the mechanisms that trigger, fuel, and quench starbursts in galaxies remain poorly understood. High-mass starburst galaxies, such as luminous and ultra luminous infrared galaxies (LIRGs and ULIRGs), are typically associated with major mergers and tidal interactions (e.g., Sanders & Mirabel 1996), suggesting that external, violent events are needed to trigger the intense star formation. In contrast, circumnuclear starbursts in isolated spiral galaxies seem to be associated with stellar bars (e.g., Kennicutt 1998; Kormendy & Kennicutt 2004), pointing to internal, secular processes. The situation is much less clear for low-mass starburst galaxies, such as

blue compact dwarfs (BCDs; Gil de Paz et al. 2003) and H II galaxies (e.g., Taylor et al. 1995), which generally lack stellar bars and spiral arms. Several authors (e.g., Ekta & Chhengalur 2010; López-Sánchez 2010; Lelli et al. 2014b) argue that external mechanisms may be important in triggering starbursts in at least some of these systems, but it is generally difficult to distinguish between dwarf-dwarf mergers, past interactions between unbound, neighboring galaxies, or cold gas accretion from the intergalactic medium. Detailed studies of the stellar and dynamical properties of starburst dwarfs, however, can provide indirect clues on the starburst trigger.

Regarding stellar properties, McQuinn et al. (2010a,b) used Hubble Space Telescope (HST) observations of 20 active starburst and post-starburst dwarfs in the Local Volume to derive accurate star-formation histories (SFHs) from fitting color-magnitude diagrams (CMDs) of resolved stellar populations. They defined a “starburst” as the period when the star-formation rate (SFR) is enhanced by at least a factor of 2 with respect to the historical average SFR in the galaxy, similar to previous prescriptions (i.e., birthrate parameter $b = \text{SFR}/\overline{\text{SFR}} \gtrsim 2$; Scalo 1986; Kennicutt et al. 2005), and found burst durations of the order of a few 100

^{*} Based on observations made with the NASA/ESA Hubble Space Telescope, and obtained from the Hubble Legacy Archive, which is a collaboration between the Space Telescope Science Institute (STScI/NASA), the Space Telescope European Coordinating Facility (ST-ECF/ESA) and the Canadian Astronomy Data Centre (CADC/NRC/CSA).

[†] E-mail: kmcquinn@astro.umn.edu

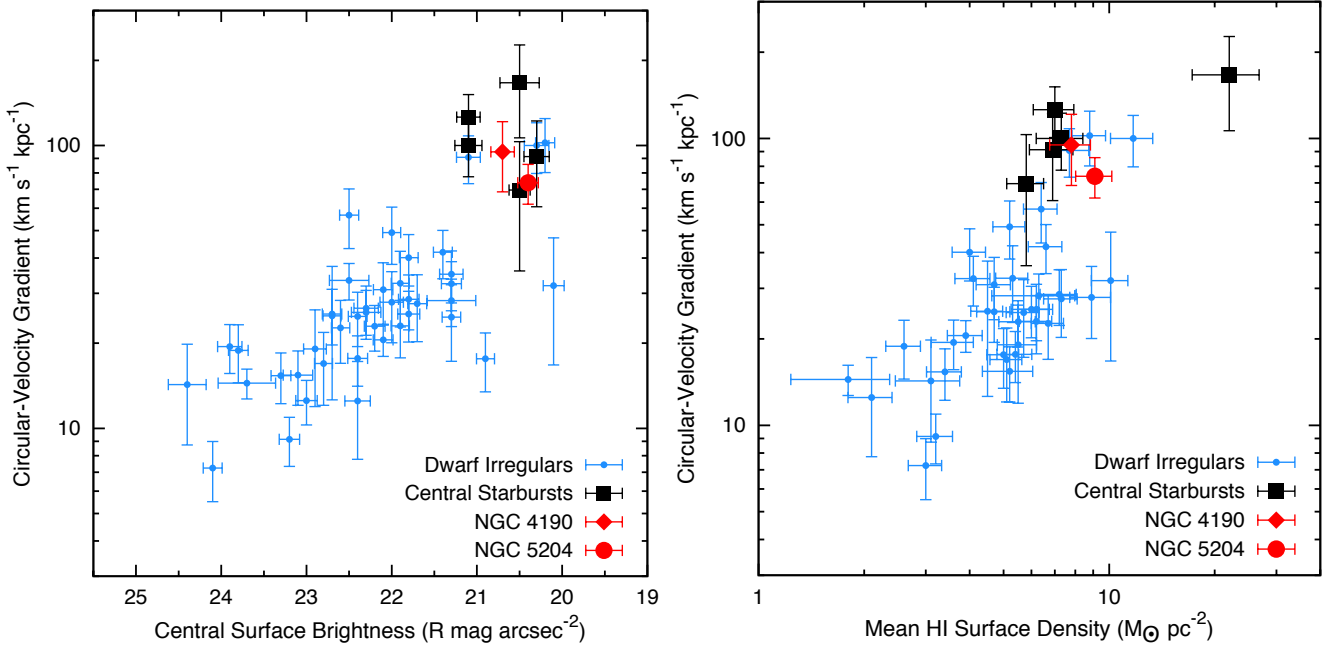


Figure 1. *Left:* Circular-velocity gradient (V_{R_d}/R_d) and central surface brightness for dwarf galaxies. *Right:* V_{R_d}/R_d versus the mean HI surface density within the optical radius. Both figures are adapted from Lelli et al. (2014). For clarity, we omit galaxies with off-centered or diffuse starbursts, such as cometary BCDs. Galaxies with a previously-identified central starburst (black symbols) lie in the upper right portion of both relations. A few dIrrs (cyan symbols) are found in the same region: two of them, NGC 4190 and NGC 5204 (red symbols), have been imaged with the HST and constitute the focus of this paper.

Myr. Moreover, McQuinn et al. (2012) studied the spatial distribution of the resolved stellar populations and found that the starburst component can cover a large fraction of the underlying host galaxy. Similar results have also been found in detailed studies of individual cases (e.g., Annibali et al. 2003, 2013). It is clear, therefore, that starbursts in dwarf galaxies are not simply stochastic, small-scale fluctuations in the SFH, but they are major events that could, in principle, dramatically affect its structure and evolution.

Regarding internal dynamics, Lelli et al. (2012a,b, 2014) found that the inner rotation curves of starburst dwarfs rise more steeply than those of typical dwarf irregulars (dIrrs; see also Meurer et al. 1998; van Zee et al. 2001), indicating that starburst galaxies have a higher central dynamical mass density (gas, stars, and dark matter). This points to a close connection between the mass distribution in a galaxy and its star formation activity. In particular, Lelli et al. (2014) considered a sample of 60 low-mass galaxies with high quality rotation curves (including dIrrs, spheroidals, and starburst dwarfs) and estimated their inner circular-velocity gradient as V_{R_d}/R_d , where R_d is the exponential scale length. As shown in Figure 1, they found that V_{R_d}/R_d correlates with the central surface brightness and the disc-averaged HI surface density, as well as the disc-averaged SFR surface density. Galaxies with central starbursts, such as BCDs, are systematically found to have high values of V_{R_d}/R_d , but there are also several “compact” dIrrs with similarly high values of V_{R_d}/R_d . The nature of these compact dIrrs is unclear: they may be the progenitors/descendants of BCDs caught in a quiescent phase, or they may be undergoing a starburst at the present time.

We identified a sample of seven “compact” dIrrs by se-

lecting galaxies in the top-right end of the $V_{R_d}/R_d - \mu_0$ relation in Figure 1 ($V_{R_d}/R_d \gtrsim 50$ km s⁻¹ kpc⁻¹, $\mu_0 \lesssim 22$ mag arcsec⁻²). Two of these (NGC 4190 and NGC 5204) have archival HST observations that meet the criteria of McQuinn et al. (2010a) for deriving SFHs. First, the galaxies were close enough such that their stellar populations were resolved by HST imaging instruments. Second, both V and I band images of the galaxy were available in the HST archive. Third, the I band observations had a minimum photometric depth of ~ 2 mag below the tip of the red giant branch; a requirement for accurately constraining the recent SFH of a galaxy (Dolphin 2002; Dohm-Palmer & Skillman 2002).

In this paper, we drive the SFHS of NGC 4190 and NGC 5204 using a CMD fitting technique. We find that both galaxies have star-formation properties that are consistent with those of known starbursts. This strongly reinforces the idea that a high central mass density (baryons and dark matter) is a key property of starburst galaxies, which must be closely linked to the mechanism that triggered the intense star-formation.

2 OBSERVATIONS AND PHOTOMETRY OF THE RESOLVED STELLAR POPULATIONS

The data for both NGC 4190 and NGC 5204 consist of archival HST imaging obtained using the Wide Field Planetary Camera 2 (WFPC2) with the F606W and F814W filters. Total integration times per filter were 2200 s for NGC 4190 and 600 s for NGC 5204. Table 1 summarizes the observations and basic properties of the systems. Figure 2 shows composite color images of both galaxies produced from the Hubble Legacy Archive pipeline. Visible in

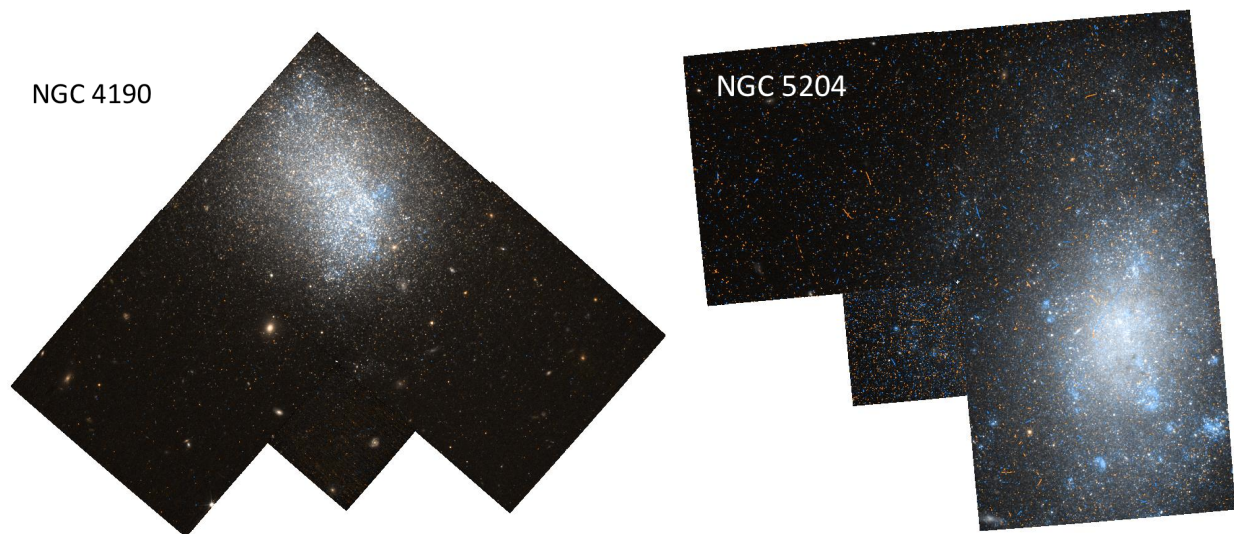


Figure 2. Composite color HST images of NGC 4190 and NGC 5204 showing both the main star forming complexes and underlying older stellar populations extending to greater radii. The images are from the Hubble Legacy Archive (Image credit: HLA, ESA, NASA) and were created by combining the F606W data (blue) and the F814W data (red). The fields are oriented North-up and East-left.

Table 1. Galaxy Properties and Observations

	NGC 4190	NGC 5204
R.A. (J2000)	12:13:44.8	13:29:36.5
Decl. (J2000)	+36:38:02.5	+58:25:07.4
Program ID	HST-GO-10905	HST-GO-8601
WFPC 2 Filters	F606W; F814W	F606W; F814W
Exposure per filter (s)	2200	600
Distance (Mpc)	2.83 ± 0.17	4.65 ± 0.53
Best-fit Distance (Mpc)	2.95 ± 0.07	4.79 ± 0.11
Foreground A_R (mag)	0.063	0.027
Best-fit A_{F606W} (mag)	0.00 ± 0.05	0.20 ± 0.05

Notes. The distances were measured using the tip of the red giant branch (TRGB) method (Tully et al. 2009; Jacobs et al. 2009; Karachentsev et al. 2003). Galactic extinction is based on the Schlafly & Finkbeiner (2011) recalibration of the Schlegel et al. (1998) dust maps. The best-fit distance and extinction values are from the CMD-fitting technique discussed in the text.

both galaxies are blue, presumably young, clustered, star-forming regions as well as a more homogeneously distributed redder, presumably older stellar population.

To ensure a uniform comparison of the star-formation properties with the starburst sample from McQuinn et al. (2010b), we processed the data and measured the SFHs with the same methodology and using the same tools as this previous study. The images were cosmic-ray cleaned and processed using the standard HST pipeline. Point spread function (PSF) photometry was performed on the individual images using HSTphot (Dolphin 2000) which is optimized for the under-sampled PSF in WFPC2 data. The raw photometry lists were filtered for well-recovered stellar-like point sources with a signal-to-noise ratio ≥ 4 and a data flag ≤ 1 . The resulting photometric catalog was further filtered for point sources with low sharpness and crowding values: |sharpness values| ≤ 0.3 and crowding values ≤ 0.5 . The sharpness parameter aids in rejecting extended, background sources. The crowding parameter aids in removing

stars whose photometric measurements are significantly affected in crowded regions by neighboring point sources. Artificial stars tests were performed on the images to measure the completeness limit and noise characteristics of the data, using the same photometry package and filtered with the same parameters.

Figure 3 shows the CMDs for both galaxies plotted to the 50% completeness level as determined from the artificial star tests. Apparent in each CMD are well-defined red giant branch (RGB) sequences populated by stars older than ~ 1 Gyr, upper main sequence (MS) stars, asymptotic giant branch (AGB) stars, and both red and blue helium burning (HeB) sequences. Stars on the HeB sequences are of intermediate mass ($M \gtrsim 3M_{\odot}$) and are burning helium in their cores (Bertelli et al. 1994). These stars are relatively young, with ages ranging from 5 to 1000 Myr. During this time period, the stars will evolve off the MS to the red HeB sequence, migrate back across the CMD to the blue HeB sequence, and finally evolve into an AGB star or end as a supernova. In contrast to RGB and MS stars, the location of an HeB star on the CMD depends uniquely on age with more massive, younger HeB stars being more luminous than less massive, older HeB stars. Observationally, HeB stars can be used as chronometers of star formation in a galaxy over the last $\lesssim 500$ Myr, when the HeB sequences typically merge into the red clump and become indistinguishable from other stars (Dohm-Palmer et al. 1997; Dohm-Palmer & Skillman 2002; McQuinn et al. 2011).

3 THE STAR FORMATION HISTORIES

The SFHs of both galaxies were measured using the numerical CMD fitting program MATCH (Dolphin 2002). This is the same SFH code used in the starburst study of McQuinn et al. (2010a) ensuring a uniform comparison of starburst metrics. Briefly, for an assumed initial mass function (IMF), MATCH uses stellar evolutionary isochrones to create

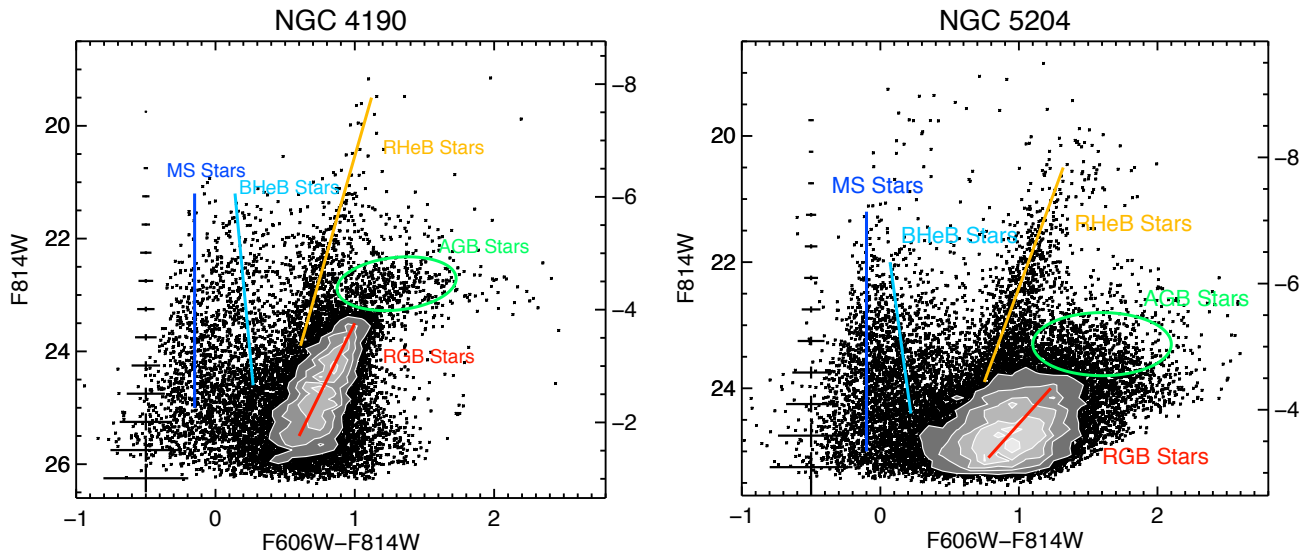


Figure 3. CMDs of NGC 4190 and NGC 5204. The RGB, MS, AGB, and red and blue HeB sequences are well-populated in both CMDs. The abundance of intermediate mass HeB stars is a clear sign of recent star formation in these galaxies.

a series of synthetic stellar populations of different ages and metallicities. The modeled CMD that is the best-fit to the observed CMD provides the most likely SFH of the galaxy. The synthetic CMDs are modeled using the photometry and recovered fractions of the artificial stars as primary inputs. The Padua stellar evolution models were used (Marigo et al. 2008) including the updated AGB tracks from Girardi et al. (2010). We assumed a Salpeter IMF (Salpeter 1955) from 0.1 to $120 M_{\odot}$ and a binary fraction of 35% with a flat secondary distribution.

Distance and extinction are free parameters fit by MATCH. The best-fit distances are reported in Table 1. They agree within the errors with independent distance measurements based on the tip of the red giant method, providing a consistency check on our results. Both foreground and internal extinction can broaden the features in a CMD, but they are expected to be low for these high-latitude, metal-poor galaxies (cf., Berg et al. 2012). Table 1 lists both the foreground extinction estimate from the dust maps of Schlegel et al. (1998) with recalibration by Schlafly & Finkbeiner (2011) and the best-fit extinction values, which includes both foreground and internal extinction at a slightly shorter wavelength. Because the photometric depth of the data does not constrain the metallicity evolution of the systems, we assumed that the chemical enrichment history, $Z(t)$, is a continuous, non-decreasing function over the lifetime of the galaxy. Uncertainties on the SFHs take into account both systematic uncertainties from the stellar evolution models (Dolphin 2012) and random uncertainties due to the finite number of stars in a CMD (Dolphin 2013).

Measuring a SFH requires sufficient information from stellar populations of different ages. At older ages, the best temporal resolution achievable is largely a function of photometric depth (Dolphin 2002; McQuinn et al. 2010a). Photometry reaching the oldest MS turn-off is required to distinguish between stars that are, for example, 12 Gyr or 10 Gyr old. Thus, with the exception of the closest galaxies in the Local Group, the temporal resolution achievable at the

earliest epochs is limited to multi-Gyr bins. At younger ages, the best temporal resolution achievable is largely a function of the number of stars in the upper part of the CMD (Dolphin 2013) with a lesser dependency on photometric depth. Thus, in galaxies with recent star formation, both the upper MS and HeB sequences can be used to constrain the recent SFHs with a much higher temporal resolution than is achievable at older times (see Section 2). The random uncertainties measured for the SFHs can help in choosing the appropriate temporal resolution for an individual data set; if the time binning is too fine, the uncertainties increase substantially. We chose the time binning for the SFHs balancing the desire for the maximum time resolution with the size of the random uncertainties. This is an improvement over the approach used in McQuinn et al. (2010a), where only systematic uncertainties were included in the SFH and a uniform time binning scheme was adopted based on the photometric depth of the data. This difference in temporal resolution will not impact our measurement of whether or not these two galaxies meet the starburst criteria because our time binning is well within the typical durations of starbursts in low-mass galaxies (a few 100 Myr; McQuinn et al. 2010b).

4 ARE THESE GALAXIES STARBURST DWARFS?

In Figure 4 we present the lifetime and recent SFHs of NGC 4190 and NGC 5204. Despite differences in the earliest epochs of star formation, both NGC 4190 and NGC 5204 show a significant rise in SFRs at recent times compared with the average SFR over the last few Gyr. This rise in recent star-formation activity is very similar to those reported by McQuinn et al. (2010b) in a sample of galaxies comprised of known starbursts.

Multiple studies have used comparisons of recent to past star-formation activity to identify starbursts, generally set-

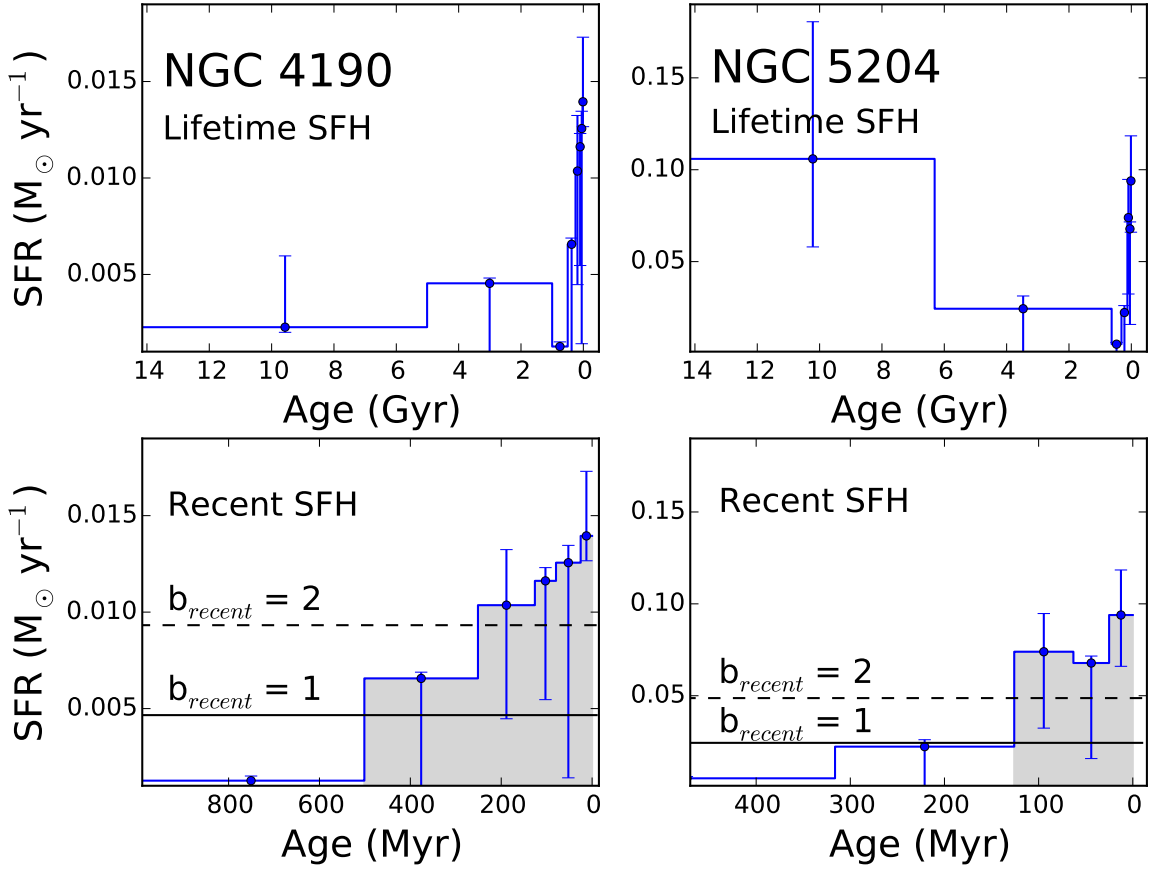


Figure 4. The lifetime SFHs of NGC 4190 and NGC 5204 are plotted in the top panels; an expanded view of the most recent SFHs are plotted in the bottom panels. Both galaxies show an increase in star-formation activity at recent times. The solid lines mark $b_{\text{recent}} = 1$, while the dotted lines mark $b_{\text{recent}} = 2$. According to the criteria of [McQuinn et al. \(2010b\)](#), both galaxies host a starburst with a duration of 380 ± 130 Myr in NGC 4190 and 100 ± 30 in NGC 5204 (shaded gray regions).

ting a birthrate parameter threshold of 2 – 3 to separate burst from non-burst activity (e.g., [Hunter & Gallagher 1986](#); [Salzer 1989](#); [Gallagher 2005](#); [Kennicutt et al. 2005](#); [Lee et al. 2009](#)). Many b measurements use recent star-formation activity measured over very short timescales of 5 – 10 Myr corresponding to the lifetimes of the most massive stars (traced by $H\alpha$ emission) and are susceptible to biases from short-duration stochastic fluctuations in individual star-forming regions. Such “flickering” star-formation activity can be $10\times$ greater than SFRs measured over longer time periods ([Lee et al. 2009](#)). The lifetime SFR averages are often based on integrated spectral measurements which can be highly uncertain ([Kennicutt et al. 1994](#)). The value of b has a strong redshift dependence with peak values as high as 30 for a wide demographic of starburst galaxies ([Brinchmann et al. 2004](#)). In studies of a narrower demographic of galaxies in the nearby universe, the average birthrate parameter based on disc-averaged SFRs for non-burst galaxies is ~ 0.5 , thus a b threshold value of 2 requires recent star-formation activity to be $4\times$ greater in starbursts than in typical non-bursting galaxies (e.g., [Kennicutt et al. 2005](#)).

[McQuinn et al. \(2010b\)](#) followed a similar convention

to identify and measure the characteristics of starburst in the SFHs, but modified the birthrate parameter to focus on the more recent evolutionary state of the host galaxies. Specifically, the birthrate parameter was defined as $b_{\text{recent}} \equiv \text{SFR} / \overline{\text{SFR}}_{t < 6 \text{ Gyr}}$, where the normalization factor is the historical average SFR within 6 Gyr. The SFRs at the earliest epochs ($t > 6$ Gyr) are not included in the historical averages, because (i) the uncertainties are larger at these older times, (ii) the generally higher levels of star-formation activity during the epoch of galaxy assembly can bias the averages, and (iii) the “recent” evolutionary state of the galaxy ($t \leq 6$ Gyr) is a more relevant baseline with which to compare the SFRs at the present epoch. This approach is only possible when measuring SFHs as other star-formation indicators are restricted to using rather uncertain lifetime average SFRs as a birthrate normalization factor. Following the convention that $b_{\text{recent}} \geq 2$ identifies a starburst, [McQuinn et al. \(2010b\)](#) further prescribed that birthrate values $\simeq 1$ can be used to identify the beginning and end of a burst. Using this metric, the duration of a starburst is measured as the amount of time $b_{\text{recent}} \geq 1$, given the $b_{\text{recent}} \geq 2$ threshold has been reached.

As seen in Figure 4, both NGC 4190 and NGC 5204 have SFRs at recent times that are higher than the b_{recent} threshold of 2 and, thus, can be considered starbursts. Moreover, the disc-averaged recent SFRs for both galaxies are elevated for at least 100 Myr, and continue to be higher than the past averages at the present day. The durations of the starbursts, shaded in grey, are $> 380 \pm 130$ Myr for NGC 4190 and $> 100 \pm 30$ Myr for NGC 5204. The peak b_{recent} values are $3.0^{+0.7}_{-0.6}$ and $3.9^{+1.0}_{-1.4}$ for NGC 4190 and NGC 5204 respectively (see Table 2). In both cases the $\overline{\text{SFR}}_{t < 6 \text{ Gyr}}$ normalization factor for the b parameters are upper limits, thus the b_{recent} values may be higher. Fluctuations in the star-formation activity and higher birthrate values over shorter time periods are presumably present in the galaxies, but the ability to measure such fluctuations is limited by the time resolution achievable with the current data. Despite this limitation, the b_{recent} values are still above the starburst threshold over multiple time bins, reinforcing the conclusion that these are starbursts rather than stochastic fluctuations in the SFRs corresponding to individual pockets of star formation. Similar to the starburst sample from McQuinn et al. (2010b), the measured durations are longer than or equivalent to the dynamical timescales of the host galaxies calculated from gas rotation speeds and effective radii (i.e., $\tau_{dyn} \equiv 2\pi R_{eff}/V_{rot}$; see Table 2). Additionally, in Table 2 we provide quantities calculated from the SFH characterizing the recent star formation including the percent of mass created in the bursts and the energy outputs of the bursts from supernovae and stellar winds estimated using the Starburst99 model (Leitherer et al. 1999). These values also fall within the ranges measured for the starburst sample in McQuinn et al. (2010b).

In summary, the star-formation characteristics in NGC 4190 and NGC 5204 are consistent with the properties measured in a larger sample of known starburst galaxies from McQuinn et al. (2010b). Indeed, these star-forming events are comprised of multiple star-forming regions with elevated levels of star formation lasting 100 Myr or longer, rather than being localized in individual, short-duration pockets of star formation.

5 DISCUSSION & CONCLUSIONS

In this study we measured the SFHs of two compact dwarf galaxies (NGC 4190 and NGC 5204) that were selected based solely on their proximity and dynamical properties: HI rotation curves with a steep rise in the inner regions ($V_{R_d}/R_d \gtrsim 50 \text{ km s}^{-1} \text{ kpc}^{-1}$). We found that the star-formation properties of both galaxies are consistent with those of previously studied, known starbursts (McQuinn et al. 2010b). This strongly reinforces the idea that the starburst activity is closely linked to the central distribution of mass (gas, stars, and dark matter), as suggested by Lelli et al. (2012a,b, 2014).

Understanding the link between starbursts and mass distribution is challenging as it depends on distinguishing between *nature* versus *nurture* scenarios: either the progenitors of starburst dwarfs are unusually compact dIrrs with steeply rising rotation curves, or there must be a mechanism that concentrates the mass in a typical dIrrs and eventually triggers the starburst (or some combination of both).

Table 2. Measured Star-Formation Characteristics

	NGC 4190	NGC 5204
Peak SFR of Burst ($M_{\odot} \text{ yr}^{-1}$)	$14^{+3}_{-1} \times 10^{-3}$	$9^{+2}_{-3} \times 10^{-2}$
Peak b_{recent} of Burst	$3.0^{+0.7}_{-0.6}$	$3.9^{+1.0}_{-1.4}$
Duration (Myr)	$\geq 380 \pm 130$	$\geq 100 \pm 30$
Total Stellar Mass (M_{\odot})	$4.4^{+3.5}_{-2.5} \times 10^7$	$9.8^{+6.3}_{-5.2} \times 10^8$
Percent Mass created in burst	$8^{+6}\%$	$0.7^{+0.5}\%$
log Energy from Burst (erg)	55.9	56.2
R_{eff} (kpc)	3.8 ± 0.2	11.3 ± 1.3
V_{rot} (km s^{-1})	25 ± 3	63 ± 4
τ_{dyn} (Myr)	93 ± 12	110 ± 14
Duration/ τ_{dyn}	4.1 ± 1.5	0.9 ± 0.3

Notes. The measured star-formation characteristics of NGC 4190 and NGC 5204. Both galaxies meet the criteria of starburst from McQuinn et al. (2010b), have starburst durations lasting 100 Myr or more, and star formation characteristics consistent with known starbursts. The stellar mass listed is the total mass formed in each galaxy (not the current stellar mass); the percent of mass formed in the bursts are upper limits. Effective radii are from Swaters & Balcells (2002); rotational velocities are from Swaters et al. (2009).

The former possibility (*nature*) has been discussed in detail by Meurer et al. (1998), van Zee et al. (2001), and Lelli et al. (2014). According to the Toomre instability criteria (Toomre 1964), a galaxy with a steeply rising rotation curve in the inner parts has a high value of the critical surface-density threshold for large-scale gravitational instabilities. As a consequence, the gas may pile up in the center over a cosmic time and reach high surface densities, until the critical threshold is reached and a starburst develops. As pointed out by Lelli et al. (2014), this does not necessarily imply a SFH characterized by short bursts and long quiescent periods, since the star formation may continue in the outer regions of the disc (along the flat part of the rotation curve) where the disc may be less stable.

The latter possibility (*nurture*) requires a mechanism (internal or external) that can transform a typical dwarf into a compact one. Several internal mechanisms have been proposed, such as mass inflows due to clump instabilities (Elmegreen et al. 2012), triaxial dark matter haloes (Bekki & Freeman 2002), or bars made of dark matter (Hunter & Elmegreen 2004). These mechanisms are generally difficult to test with observations; to date there is no direct evidence that they may actually take place in dwarf galaxies. External mechanisms, instead, can be investigated using deep optical imaging (e.g., López-Sánchez et al. 2010; Martínez-Delgado et al. 2012) or HI observations (e.g., Ekta et al. 2008; Ekta & Chengalur 2010). Recently, Lelli et al. (2014b) studied the distribution and kinematics of the HI gas in the *outer regions* of 18 starburst dwarfs, and found that they systematically have more asymmetric/disturbed HI morphologies than typical dIrrs. As discussed in Lelli et al. (2014b), these outer HI asymmetries cannot be the result of massive gas outflows (see also Lelli et al. 2014a), but point to external mechanisms triggering the starbursts. Obvious possibilities are interaction/mergers between dwarf galaxies or cold gas accretion from the intergalactic medium. NGC 4190 and NGC 5204 qualitatively fit this picture: the HI map of NGC 4190 shows pronounced asymmetries in

the outer parts, while NGC 5204 has a strongly warped HI disc (see Appendix B of Swaters et al. 2002). Interestingly, numerical simulations suggest that the formation of a compact mass distribution may be easily explained by interactions/mergers between gas-rich dwarfs (e.g., Bekki 2008), but a detailed comparison between simulations and observations is still lacking.

Regardless of the *nature* versus *nurture* issue, it would be interesting to search for the descendants of starburst dwarfs, or post-starburst dwarfs, among quiescent compact dwarfs. If the link between mass concentration and starbursts is confirmed, it would also have important implications for statistical estimates of burst duty cycles based on large galaxy surveys (e.g., Lee et al. 2009), given that only compact dIrrs would repeatedly experience starburst episodes during their lifetime. Moreover, it would bring into question whether stellar feedback from starbursts can really transform central dark matter cusps (predicted by N-body simulations) into the observed cores (e.g., Governato et al. 2010; Oh et al. 2011; Governato et al. 2012; Teyssier et al. 2013; Garrison-Kimmel et al. 2013; Di Cintio et al. 2014; Brooks & Zolotov 2014; Ogiya et al. 2014; Madau et al. 2014). SFHs of other compact dIrrs from new HST imaging would clarify whether dIrrs with steeply-rising rotation curves are necessarily experiencing a starburst (like NGC 4190 and NGC 5204) or whether some of them can be considered descendants of starburst dwarfs. This would shed new light on the future evolution of starburst dwarfs and firmly establish the link between star formation and mass distribution for a large galaxy sample.

ACKNOWLEDGMENTS

FL thanks Filippo Fraternali, Renzo Sancisi, and Marc Verheijen for many enlightening discussions about the dynamics of dwarf galaxies. This research made use of NASA’s Astrophysical Data System and the NASA/IPAC Extragalactic Database (NED) which is operated by the Jet Propulsion Laboratory, California Institute of Technology, under contract with the National Aeronautics and Space Administration.

REFERENCES

Annibali F., Cignoni M., Tosi M., van der Marel R. P., Aloisi A., Clementini G., Contreras Ramos R., Fiorentino G., Marconi M., Musella I., 2013, ArXiv e-prints
 Annibali F., Greggio L., Tosi M., Aloisi A., Leitherer C., 2003, *AJ*, 126, 2752
 Bekki K., 2008, *MNRAS*, 388, L10
 Bekki K., Freeman K. C., 2002, *ApJL*, 574, L21
 Berg D. A., Skillman E. D., Marble A. R., van Zee L., Engelbracht C. W., Lee J. C., Kennicutt Jr. R. C., Calzetti D., Dale D. A., Johnson B. D., 2012, *ApJ*, 754, 98
 Bertelli G., Bressan A., Chiosi C., Fagotto F., Nasi E., 1994, *A&A Supplement Series*, 106, 275
 Brinchmann J., Charlot S., White S. D. M., Tremonti C., Kauffmann G., Heckman T., Brinkmann J., 2004, *MNRAS*, 351, 1151
 Brooks A. M., Zolotov A., 2014, *ApJ*, 786, 87

Di Cintio A., Brook C. B., Macciò A. V., Stinson G. S., Knebe A., Dutton A. A., Wadsley J., 2014, *MNRAS*, 437, 415
 Dohm-Palmer R. C., Skillman E. D., 2002, *AJ*, 123, 1433
 Dohm-Palmer R. C., Skillman E. D., Saha A., Tolstoy E., Mateo M., Gallagher J., Hoessel J., Chiosi C., Dufour R. J., 1997, *AJ*, 114, 2527
 Dolphin A. E., 2000, *PASP*, 112, 1383
 Dolphin A. E., 2002, *MNRAS*, 332, 91
 Dolphin A. E., 2012, *ApJ*, 751, 60
 Dolphin A. E., 2013, *ApJ*, 775, 76
 Ekta Chengalur J. N., Pustilnik S. A., 2008, *MNRAS*, 391, 881
 Ekta B., Chengalur J. N., 2010, *MNRAS*, 403, 295
 Elmegreen B. G., Zhang H.-X., Hunter D. A., 2012, *ApJ*, 747, 105
 Gallagher III J. S., 2005, in de Grijs R., González Delgado R. M., eds, *Starbursts: From 30 Doradus to Lyman Break Galaxies Vol. 329 of Astrophysics and Space Science Library*, Starbursts in the Evolving Universe: A Local Perspective. p. 11
 Garrison-Kimmel S., Rocha M., Boylan-Kolchin M., Bullock J. S., Lally J., 2013, *MNRAS*, 433, 3539
 Gil de Paz A., Madore B. F., Pevunova O., 2003, *ApJS*, 147, 29
 Girardi L., Williams B. F., Gilbert K. M., Rosenfield P., Dalcanton J. J., Marigo P., Boyer M. L., Dolphin A., Weisz D. R., Melbourne J., Olsen K. A. G., Seth A. C., Skillman E., 2010, *ApJ*, 724, 1030
 Governato F., Brook C., Mayer L., Brooks A., Rhee G., Wadsley J., Jonsson P., Willman B., Stinson G., Quinn T., Madau P., 2010, *Nature*, 463, 203
 Governato F., Zolotov A., Pontzen A., Christensen C., Oh S. H., Brooks A. M., Quinn T., Shen S., Wadsley J., 2012, *MNRAS*, 422, 1231
 Hunter D. A., Elmegreen B. G., 2004, *AJ*, 128, 2170
 Hunter D. A., Gallagher III J. S., 1986, *PASP*, 98, 5
 Jacobs B. A., Rizzi L., Tully R. B., Shaya E. J., Makarov D. I., Makarova L., 2009, *AJ*, 138, 332
 Karachentsev I. D., Makarov D. I., Sharina M. E., Dolphin A. E., Grebel E. K., Geisler D., Guhathakurta P., Hodge P. W., Karachentseva V. E., Sarajedini A., Seitzer P., 2003, *A&A*, 398, 479
 Kennicutt R. C., Lee J. C., Akiyama S., Funes J. G., Sakai S., 2005, in Hüttmeister S., Manthey E., Bomans D., Weis K., eds, *The Evolution of Starbursts Vol. 783 of American Institute of Physics Conference Series*, The Demographics of Starburst Galaxies. pp 3–16
 Kennicutt Jr. R. C., 1998, *ARA&A*, 36, 189
 Kennicutt Jr. R. C., Tamblyn P., Congdon C. E., 1994, *ApJ*, 435, 22
 Kormendy J., Kennicutt Jr. R. C., 2004, *ARA&A*, 42, 603
 Lee J. C., Gil de Paz A., Tremonti C., Kennicutt Jr. R. C., Salim S., Bothwell M., Calzetti D., Dalcanton J., Dale D., Engelbracht C., Funes S. J. J. G., Johnson B., Sakai S., Skillman E., van Zee L., Walter F., Weisz D., 2009, *ApJ*, 706, 599
 Leitherer C., Schaerer D., Goldader J. D., Delgado R. M. G., Robert C., Kune D. F., de Mello D. F., Devost D., Heckman T. M., 1999, *ApJS*, 123, 3
 Lelli F., Fraternali F., Verheijen M., 2014, *A&A*, 563, A27
 Lelli F., Verheijen M., Fraternali F., 2014a, *A&A*, 566, A71

- Lelli F., Verheijen M., Fraternali F., 2014b, *MNRAS*, 445, 1694
- Lelli F., Verheijen M., Fraternali F., Sancisi R., 2012a, *A&A*, 537, A72
- Lelli F., Verheijen M., Fraternali F., Sancisi R., 2012b, *A&A*, 544, A145
- López-Sánchez Á. R., 2010, *A&A*, 521, A63
- López-Sánchez A. R., Koribalski B., van Eymeren J., Esteban C., Popping A., Hibbard J., 2010, in Verdes-Montenegro L., Del Olmo A., Sulentic J., eds, *Galaxies in Isolation: Exploring Nature Versus Nurture Vol. 421 of Astronomical Society of the Pacific Conference Series, The Environment of Nearby Blue Compact Dwarf Galaxies*. p. 65
- Madau P., Shen S., Governato F., 2014, *ApJL*, 789, L17
- Marigo P., Girardi L., Bressan A., Groenewegen M. A. T., Silva L., Granato G. L., 2008, *A&A*, 482, 883
- Martínez-Delgado D., Romanowsky A. J., Gabany R. J., Annibali F., Arnold J. A., Fliri J., Zibetti S., et al. 2012, *ApJL*, 748, L24
- McQuinn K. B. W., Skillman E. D., Cannon J. M., Dalcanton J., Dolphin A., Hidalgo-Rodríguez S., Holtzman J., Stark D., Weisz D., Williams B., 2010a, *ApJ*, 721, 297
- McQuinn K. B. W., Skillman E. D., Cannon J. M., Dalcanton J., Dolphin A., Hidalgo-Rodríguez S., Holtzman J., Stark D., Weisz D., Williams B., 2010b, *ApJ*, 724, 49
- McQuinn K. B. W., Skillman E. D., Dalcanton J. J., Cannon J. M., Dolphin A. E., Holtzman J., Weisz D. R., Williams B. F., 2012, *ApJ*, 759, 77
- McQuinn K. B. W., Skillman E. D., Dalcanton J. J., Dolphin A. E., Holtzman J., Weisz D. R., Williams B. F., 2011, *ApJ*, 740, 48
- Meurer G. R., Staveley-Smith L., Killeen N. E. B., 1998, *MNRAS*, 300, 705
- Ogiya G., Mori M., Ishiyama T., Burkert A., 2014, *MNRAS*, 440, L71
- Oh S.-H., Brook C., Governato F., Brinks E., Mayer L., de Blok W. J. G., Brooks A., Walter F., 2011, *AJ*, 142, 24
- Salpeter E. E., 1955, *ApJ*, 121, 161
- Salzer J. J., 1989, *ApJ*, 347, 152
- Sanders D. B., Mirabel I. F., 1996, *ARA&A*, 34, 749
- Scalo J. M., 1986, *Fundamentals of Cosmic Physics*, 11, 1
- Schlafly E. F., Finkbeiner D. P., 2011, *ApJ*, 737, 103
- Schlegel D. J., Finkbeiner D. P., Davis M., 1998, *ApJ*, 500, 525
- Swaters R. A., Balcells M., 2002, *A&A*, 390, 863
- Swaters R. A., Sancisi R., van Albada T. S., van der Hulst J. M., 2009, *A&A*, 493, 871
- Swaters R. A., van Albada T. S., van der Hulst J. M., Sancisi R., 2002, *A&A*, 390, 829
- Taylor C. L., Brinks E., Grashuis R. M., Skillman E. D., 1995, *ApJS*, 99, 427
- Teyssier R., Pontzen A., Dubois Y., Read J. I., 2013, *MNRAS*, 429, 3068
- Toomre A., 1964, *ApJ*, 139, 1217
- Tully R. B., Rizzi L., Shaya E. J., Courtois H. M., Makarov D. I., Jacobs B. A., 2009, *AJ*, 138, 323
- van Zee L., Salzer J. J., Skillman E. D., 2001, *AJ*, 122, 121